Generation and Annihilation of Topologically Protected Bound States in the Continuum and Circularly Polarized States by Symmetry Breaking

Taiki Yoda[1] and Masaya Notomi[1,2,3,*]

[1]NTT Basic Research Laboratories, NTT Corporation, 3-1 Morinosato-Wakamiya, Atsugi-shi, Kanagawa 243-0198, Japan
[2]Department of Physics, Tokyo Institute of Technology, 2-12-1 Ookayama, Meguro-ku, Tokyo 152-8550, Japan
[3]Nanophotonics Center, NTT Corporation, 3-1, Morinosato-Wakamiya, Atsugi-shi, Kanagawa 243-0198, Japan

(Received 23 January 2020; accepted 22 June 2020; published 30 July 2020; corrected 20 January 2021)

We demonstrate by breaking the C_6 symmetry for higher-order at-Γ bound states in the continuum (BICs) with topological charge −2 in photonic crystals (i) deterministic generation of off-Γ BICs from the at-Γ BIC and (ii) a variety of pair-creation and annihilation processes of circularly polarized states with opposite topological charges and the same handedness. To explain these phenomena, we introduce the handedness-wise topological charge quantized to a half-integer. The handedness-wise charge gives a unified picture of various phenomena involving BICs and circularly polarized states.

DOI: 10.1103/PhysRevLett.125.053902

Introduction.—The concept of topology has been widely applied to photonic systems [1–3]. Various intriguing phenomena associated with nontrivial Bloch wave functions have been studied extensively. Recent studies suggest that far-field polarization vector fields radiated from photonic crystals (PhCs), also determined from Bloch wave functions, possess intriguing topological natures, including bound states in the continuum (BICs) [4–11], band degeneracies [8,12,13], and circularly polarized states (CPSs) [14–16].

BICs are resonances with infinite quality factors, although their frequencies fall inside continuous spectrum of radiation modes. At the Γ point, BICs result from the symmetry mismatch between PhC modes and radiative plane waves; this type of BIC is called an at-Γ BIC or symmetry-protected BIC. Because of the symmetry protection, the occurrence of at-Γ BICs does not depend on structural parameters. Interestingly, it was found that BICs can also exist at finite wave vectors apart from the symmetry point in a certain type of PhC, called off-Γ BICs or topologically protected BICs [4,5]. Off-Γ BICs have attracted much attention to applications such as on-chip beam steering [17,18] and generation of directive vector beams [19–21]. Moreover, off-Γ BICs can propagate without radiation loss even though their frequency is above the light line [22–24]. In spite of these interesting properties, a systematic way to generate off-Γ BICs is still lacking. Previously, off-Γ BICs have been formed by accidental cancellation of outgoing waves, and thus they are sometimes called *accidental* BICs. In stark contrast to at-Γ BICs, we must tune structural parameters carefully to generate off-Γ BICs.

CPSs have other polarization singularities for far-field polarization vector fields in PhCs without C_2 symmetry [14–16]. CPSs are resonances with *finite* quality factors, and they couple to circularly polarized radiative plane waves. Both BICs and CPSs are polarization vortex centers in the reciprocal space and carry quantized topological charges ν. The charge ν is an integer for BICs and a half-integer for CPSs. So far, most previous studies dealt with topological processes involving BICs with $\nu = \pm 1$ such as annihilation of two BICs with opposite charges.

In this study, we focus on at-Γ BICs with a higher topological charge and demonstrate that a variety of interesting phenomena arise from breaking the crystal symmetry of PhCs having a higher-order charge. First, we demonstrate that this leads to a systematic way to generate off-Γ BICs. We show that an at-Γ BIC with $\nu = -2$ in triangular-lattice PhCs can be split into two off-Γ BICs by breaking C_6 symmetry but preserving C_2 symmetry. These off-Γ BICs can be *deterministically* generated by an infinitesimal perturbation without fine-tuning parameters. Second, we demonstrate a wide variety of ways to generate and annihilate CPSs. We show that a perturbation breaking the C_2 symmetry but preserving C_3 symmetry generates six CPSs and that a variety of pair creations and annihilations of CPSs having *opposite charges* and the *same handedness* can be achieved through symmetry control starting from the at-Γ BIC with $\nu = -2$. Importantly, we show that all these phenomena are governed by the conservation of topological charges. Although previous studies have already pointed out the importance of the charge conservation in far-field topological photonics [5] with an analogy to singular optics for beam propagation [25–27], it is still not clear how far this law can hold for PhCs. Actual examples where the charge conservation plays a key role are limited to the case where $|\nu|$ of BIC is 1 [4–16], and the applicability of the conservation has not been fully explored. We introduce handedness-wise charges ($\nu_\pm$) and clearly prove that they can fully explain a variety of ways to generate and annihilate BICs and CPSs.

First of all, let us begin with describing two-dimensional (2D) PhC slabs with a finite thickness [28]. Above the light line and below the diffraction limit, a nondegenerate eigenmode with an in-plane wave vector $\mathbf{k}_{||} = (k_x, k_y)$ generally couples to a propagating plane wave with the same $\mathbf{k}_{||}$ and a polarization vector $\mathbf{d}(\mathbf{k}_{||})$ in the sp plane [4,5]. To discuss the topology in $\mathbf{k}_{||}$ space, we introduce a 2D polarization vector projected onto the xy plane, $\mathbf{d}'(\mathbf{k}_{||}) = d'_x(\mathbf{k}_{||})\hat{x} + d'_y(\mathbf{k}_{||})\hat{y}$ (see Sec. S1 in the Supplemental Material [29]). The topological charge of the polarization singularities for $\mathbf{d}'(\mathbf{k}_{||})$ is defined by [5–16,25–27]

$$\nu = \frac{1}{2\pi}\oint_C d\mathbf{k}_{||} \cdot \nabla_{\mathbf{k}_{||}} \phi(\mathbf{k}_{||}), \qquad (1)$$

where C is a closed loop in the $\mathbf{k}_{||}$ space, $\phi(\mathbf{k}_{||}) = \frac{1}{2}\arg[S_1(\mathbf{k}_{||}) + iS_2(\mathbf{k}_{||})]$ is the angle between its long axis of the polarization ellipse and the x axis, and $S_i(\mathbf{k}_{||})$ is the Stokes parameter of $\mathbf{d}'(\mathbf{k}_{||})$. ν describes how many times the polarization ellipse of the polarization vector winds along a loop C. The charge ν is an integer if a loop C encloses a BIC where $S_1 = S_2 = S_3 = 0$ [5–11]. The charge ν is a half-integer if a loop C encloses a CPS where $S_1 = S_2 = 0$ and $S_3 = \pm 1$ [14–16]. The half-integer nature of ν originates from the fact that the polarization ellipse is described by the real symmetric tensor [25,26]. Equation (1) takes the same form as quantized Berry phases in PT-symmetric systems because both the polarization ellipse and PT-symmetric system are described by real symmetric matrices (see Sec. S3 in the Supplemental Material [29]).

Generation of off-Γ BIC from at-Γ BIC.—The possible charge of an at-Γ BIC is determined by the eigenvalues of the rotational symmetry of the system [5]. Here we particularly focus on an at-Γ BIC with a symmetry-protected higher-order charge (see Ref. [43] and Sec. S4 in the Supplemental Material [29]). Although at-Γ BICs with $\nu = \pm 1$ cannot be moved by perturbations that lower the symmetry of a PhC but preserve C_2 symmetry, we find that at-Γ BICs with $|\nu| \geq 2$ can be moved by splitting into off-Γ BICs. The perturbations reduce the charge of the BIC and then the change of ν generates new off-Γ BICs. Since this splitting relies on the charge conservation and crystalline symmetry, the generation of off-Γ BICs can be controlled by systematic deformation of the lattice symmetry in contrast to the generation of off-Γ BICs by an accidental fine-tuning of structural parameters [5]. It is worth noting that, although the destruction of at-Γ BICs by reducing symmetry has been reported [44,45], the splitting of an at-Γ BIC into off-Γ BICs has not been pointed out in previous works.

To verify the splitting of the at-Γ BIC, we numerically investigate a triangular-lattice PhC slab of circular air holes with lattice constant a, hole radius $r = 0.28a$, slab thickness $h = 0.38a$, and refractive index $n_0 = 3.48$ [Fig. 1(a)] by the finite-element method. The lowest TE-like band at the Γ point belongs to the representation B_1 of the C_{6v} point group [Figs. 1(b) and 1(c)] and thus becomes an at-Γ BIC with $\nu = -2 + 6n$ [5]. The calculated quality factor and polarization vector of the lowest TE-like band are plotted in Fig. 1(d). We find that the quality factor (Q) diverges at the Γ point and that the polarization vector winds twice around it. We also plot nodal lines of d'_x and d'_y in Fig. 1(d) and find that both nodal lines are doubly degenerate at the Γ point. These results demonstrate that a BIC with charge −2 exists at the Γ point [5,9,19].

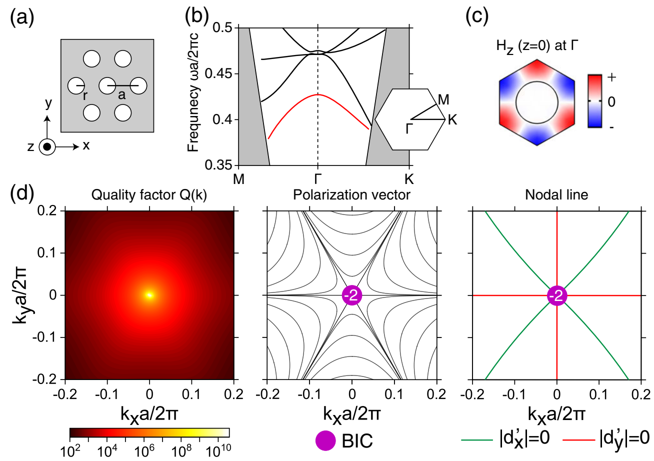

FIG. 1. (a) Schematics of a PhC slab with a triangular lattice of circular air holes. (b) Calculated TE-like band structure. The red line is the lowest TE-like band. The gray region indicates a region below the light line. The inset is the first Brillouin zone. (c) Mode profile in the unit cell for the lowest TE-like band. (d) Calculated quality factor (left), polarization vector (middle), and nodal lines of d'_x and d'_y (right). The projected polarization vector is represented by the line field tangent to the long axis of the polarization ellipse [8,10–16,25,26].

Next, we introduce perturbations breaking the C_6 symmetry but preserving the C_2 symmetry. Here we slightly vary the angle θ between two translational vectors defined in Fig. 2(a) [46]. When θ is deviated from 60° (corresponding to uniaxial deformation in the triangular lattice), the symmetry of the eigenmode for the lowest TE-like band at the Γ point is reduced to the B_1 representation of the C_{2v} point group. As mentioned before, we can expect that the perturbation split the original BIC with $\nu = -2$ into two off-Γ BICs with $\nu = -1$ through the charge conservation. We numerically calculate Q for $\theta = 58°$ and $\theta = 62°$ [Figs. 2(b) and 2(c) left]. We can observe two high-Q states at finite wave vectors on a mirror-invariant axis ($k_x = 0$ or $k_y = 0$). To prove that these states are exact BICs, not quasi-BICs [47,48], we also plot the polarization vector and nodal lines of d'_x and d'_y in Figs. 2(b) and 2(c). The polarization ellipse winds by -2π around the high-Q states [Figs. 2(b) and 2(c) middle]. This plot shows that

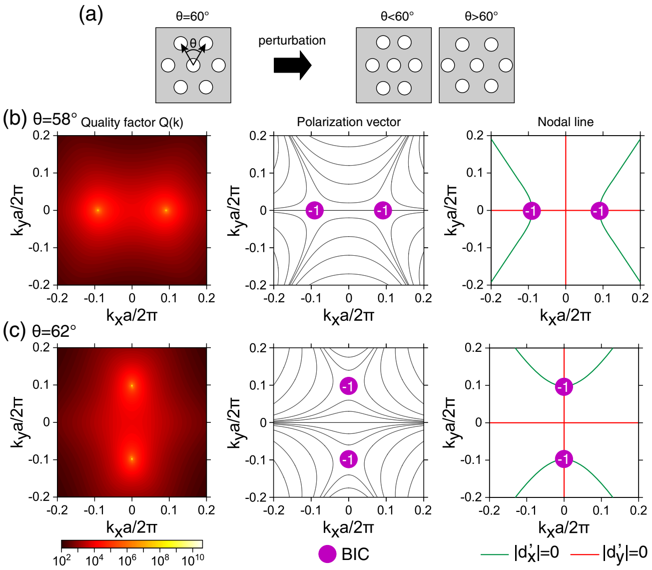

FIG. 2. (a) Definition of the angle θ and schematics of perturbed PhCs. (b),(c) Calculated quality factor (left), polarization vector (middle), and nodal lines of d'_x and d'_y (right) for (b) $\theta = 58°$ and (c) $\theta = 62°$.

the perturbation splits the degeneracy of the nodal lines at the Γ point. In addition, the nodal lines intersect each other at the high-Q states [Figs. 2(b) and 2(c) right], where the polarization vector vanishes [4,5,30]. These results unambiguously verify that the at-Γ BIC with $\nu = -2$ is split into the two exact off-Γ BICs with $\nu = -1$ by the uniaxial deformation. This finding shows that there is always a systematic way to generate off-Γ BICs from higher-order at-Γ BICs.

Conventional off-Γ BICs can exist only at a certain range of the structural parameters. In Sec. S5 in the Supplemental Material [29], we demonstrate that off-Γ BICs do not exist when $h < 0.97a$ for the PhC with $r = 0.28a$, $n_0 = 3.48$, and $\theta = 60°$. This contrasts with the present deterministic off-Γ BICs that always exist at any thickness because the existence of at-Γ BICs is guaranteed by the symmetry. Furthermore, we have confirmed that it is possible to widely change the wave vector of off-Γ BICs by simply varying θ, as shown in Sec. S6 in the Supplemental Material [29]. The result shows that one can widely change the emission angle of polarization vortex beams generated from BICs between 0° and 90°, which will be promising for vortex-beam steering devices.

Generation and annihilation of CPSs.—Recently, generation of two CPSs from splitting a BIC with charge ±1 in PhCs by breaking spatial symmetries was reported [14–16]. Here we demonstrate that starting from a higher-order at-Γ BIC with charge −2, we are able to observe far richer phenomena, including various pair creations and annihilations.

Before showing the actual examples, we point out that ν defined by Eq. (1) cannot fully describe the processes involved with CPSs because it does not contain the Stokes parameter S_3. To overcome this difficulty, we express $\mathbf{d}'(\mathbf{k}_{||})$ in terms of the circular basis [26,27,49],

$$\mathbf{d}'(\mathbf{k}_{||}) = d'_+(\mathbf{k}_{||})\mathbf{e}_+ + d'_-(\mathbf{k}_{||})\mathbf{e}_-, \tag{2}$$

where $\mathbf{e}_\pm = (\hat{x} \pm i\hat{y})/\sqrt{2}$ and $d'_\pm(\mathbf{k}_{||}) = [d'_x(\mathbf{k}_{||}) \mp i d'_y(\mathbf{k}_{||})]/\sqrt{2}$. In this basis, zeros of $d'_\pm(\mathbf{k}_{||})$ correspond to CPSs. When both $d'_+(\mathbf{k}_{||})$ and $d'_-(\mathbf{k}_{||})$ are simultaneously zero, a eigenmode turns into a BIC. By writing $d'_\pm(\mathbf{k}_{||})$ as $d'_\pm(\mathbf{k}_{||}) = |d'_\pm| e^{i\alpha_\pm}$, we introduce an integer [26,27],

$$\nu_\pm = \frac{1}{2\pi} \oint_C d\mathbf{k}_{||} \cdot \nabla_{\mathbf{k}_{||}} \alpha_\pm(\mathbf{k}_{||}). \tag{3}$$

$\nu_\pm$ is a finite integer when a loop C encloses the zeros of $d'_\pm(\mathbf{k}_{||})$. ν and $\nu_\pm$ are related by

$$\nu = \frac{1}{2}(\nu_- - \nu_+) \tag{4}$$

because $\phi(\mathbf{k}_{||})$ is given by $\phi(\mathbf{k}_{||}) = \frac{1}{2}\arg(d'^*_+ d'_-)$. It follows from Eq. (4) that $\nu_\pm$ is a handedness-wise charge, meaning the winding number weighted by its handedness S_3. Assuming the conservation for ν and $\nu_\pm$, a BIC with $\nu = \pm 1$ can be regarded as the superposition of two CPSs with $(\nu_+, \nu_-) = \pm(-1, +1)$, which indeed correctly explains the observation that a perturbation breaking C_2 symmetry splits the BIC into two CPSs with the *same topological charge* ν and *opposite handedness* S_3 [14–16]. Furthermore, a CPS with $\nu_\pm = +1$ can be removed through collision with another CPS with $\nu_\pm = -1$, i.e., *opposite topological charge* ν and *same handedness* S_3. The introduction of $\nu_\pm$ consistently explains the splitting of a BIC into two CPSs and predicts the rule for pair annihilation of two CPSs.

Here we examine actual examples. We break the C_2 symmetry by deforming circular air holes into triangular air holes with a side length of $d = 0.75a$, a slab thickness of $h = 0.38a$, and $\theta = 60°$ [Fig. 3(a)]. This deformation reduces the crystalline symmetry from C_{6v} to C_{3v}, which allows CPSs. The perturbation does not break the at-Γ BIC because C_3 symmetry still protects an at-Γ BIC with $\nu = 1 + 3n$ [5]. We plot the calculated polarization vector for the lowest TE-like band [Fig 3(e)]. The polarization ellipse now winds only once in the opposite direction around the Γ point, indicating ν of the at-Γ BIC changes from −2 to +1. Since the present PhC is no longer invariant under C_2 symmetry, the change of ν may generate six CPSs with $\nu = -1/2$ through the charge conservation. This prediction is indeed confirmed in Fig. 3(e). We find that the polarization ellipse winds by $-\pi$ around six CPSs. The

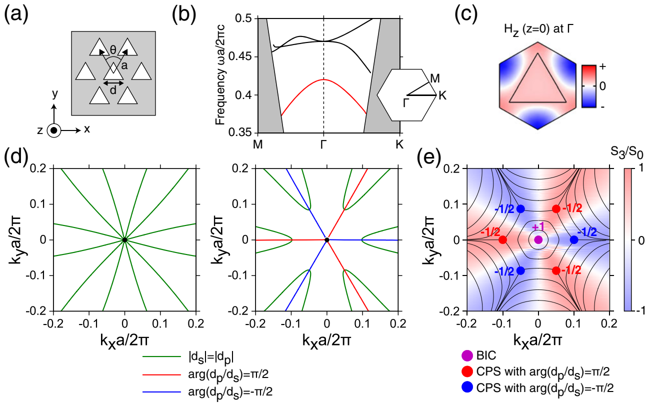

FIG. 3. (a) A triangular-lattice PhC with triangular air holes. (b) Calculated TE-like band structure. (c) Mode profile in the unit cell for the lowest TE-like band. (d) Lines for $|d_s| = |d_p|$ (green) and $\delta = \pm\pi/2$ (red and blue) for PhCs with circular (left) and triangular (right) holes. (e) Calculated polarization vector and normalized Stokes parameter $S_3/S_0 = 2|d_s||d_p| \sin\delta/(|d_s|^2 + |d_p|^2)$. The attached numbers denote topological charges ν.

half-winding indicates $\nu = -1/2$. Among the six CPSs, three CPSs are left-handed with $\delta = \pi/2$ [$\delta \equiv \arg(d_p/d_s)$] and the others are right-handed with $\delta = -\pi/2$, which is explained by the conservation of $\nu_\pm$.

For better understanding, we plot lines for $|d_s| = |d_p|$ (Lines A) and $\delta = \pm\pi/2$ (Lines B). For the circular-hole PhC [Fig. 3(d) left], Lines A emerge between the lines for $d_s = 0$ and $d_p = 0$ [30]. Lines B do not exist due to the C_2 symmetry. For the triangular-hole PhC [Fig. 3(d) right], the degeneracy of Lines A at the Γ point is lifted, and Lines B emerge. The six intersections between Lines A and B correspond to CPSs, which guarantees the topological protection of CPSs in a similar way to that of BICs [5].

Finally, we vary the angle θ from 60° to introduce the uniaxial deformation. It is expected from the conservation of $\nu_\pm$ that perturbations breaking the C_3 symmetry splits the at-Γ BIC into two CPSs with the same charge $+1/2$ and opposite handedness [Figs. 4(a) and 4(d)]. For $\theta > 60°$ ($\theta < 60°$), the CPS with $\delta = -\pi/2$ splits in the direction of $k_x > 0$ ($k_x < 0$). As the perturbation is increased, two CPSs with opposite charges and the same handedness approach [Figs. 4(b) and 4(e)] and eventually collide with each other, resulting in pair annihilation of CPSs [Figs. 4(c) and 4(f)]. Finally, the two pairs of CPSs with charge $-1/2$ and opposite handedness survive. Note that these two pair of CPSs can be regarded as generated from the off-Γ BICs in Figs. 2(b) and 4(c) as a result of breaking C_2 symmetry. Let us point out that all through these processes [Figs. 4(a)–(f)], the topological charges $\nu_\pm$ are consistently conserved and prove that conventional topological charges ν are not sufficient for explaining the results.

In conclusion, we have demonstrated deterministic generation of off-Γ BICs and a variety of ways to generate and annihilate CPSs by using a single at-Γ BIC with charge -2 and perturbations that lower the symmetry of PhCs. All processes are successfully explained by the charge conservation for handedness-wise topological charges $\nu_\pm$. This clearly demonstrates the wide applicability of the charge conservation of $\nu_\pm$ for far-field topological photonics by PhCs and guarantees the stability of their polarization singularities in parameter spaces. As another possibility, the accidental merging of two CPSs with opposite handedness and opposite charges causes accidental BICs without any in-plane symmetry [16]. The merging of two CPSs with

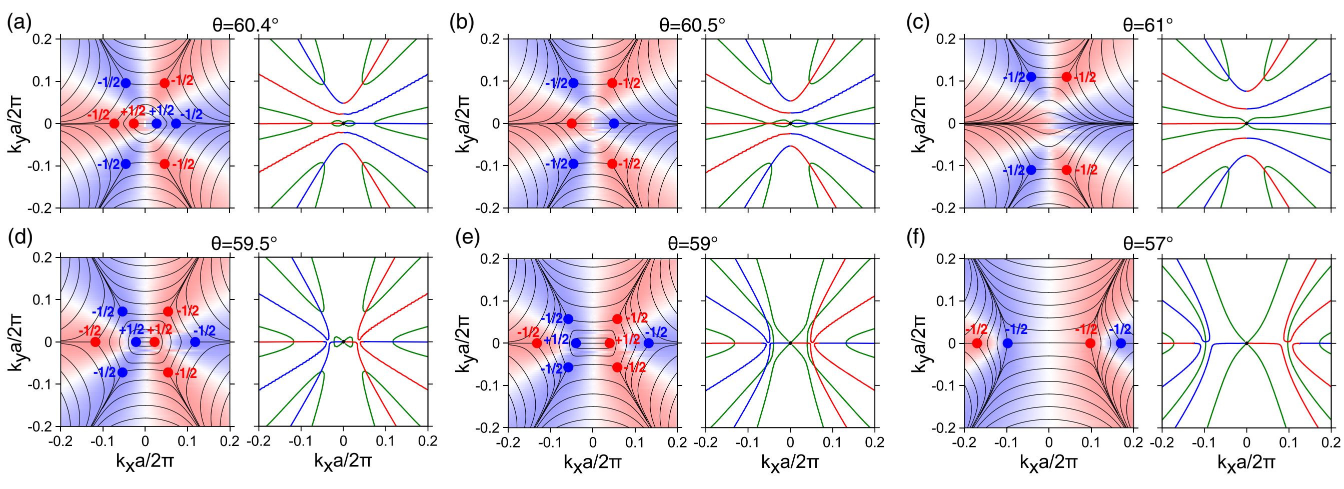

FIG. 4. Evolution of CPSs. In (a)–(f), left panels show calculated polarization vector and normalized Stokes parameter S_3/S_0, and right panels show lines for $|d_s| = |d_p|$ (green) and $\delta = \pm\pi/2$ (red and blue). For (a) $\theta = 60.4°$ and (d) $\theta = 59.5°$, the at-Γ BIC ($\nu = +1$) split into two CPSs ($\nu = +1/2$). For (b) $\theta = 60.5°$ and (e) $\theta = 59°$, two CPSs with opposite charges and the same handedness approach each other. For (c) $\theta = 61°$ and (f) $\theta = 57°$, two CPSs with opposite charges and the same handedness collide, and then they annihilate by the collision. In (a)–(f), one of five lines for $\delta = \pm 1/2$ is pinned at the Γ point due to σT symmetry (see Sec. S2 in the Supplemental Material [29]).

the same handedness and same charge may generate a higher-order CPS with $|\nu| \geq 1$. Practically, our findings suggest a novel method for creating various polarization singularities of far-field radiations such as circularly polarized light emission [50–52]. This novel way for generating off-Γ BICs will be especially promising for on-chip vortex-beam steering [17,18] and dynamic tuning of a quality factor [44].

We thank Yuto Moritake and Kenta Takata for helpful discussions. This work was supported by Japan Society for the Promotion of Science (KAKENHI JP15H05735).

*notomi@phys.titech.ac.jp

[1] L. Lu, J. D. Joannopoulos, and M. Soljačić, Topological photonics, Nat. Photonics **8**, 821 (2014).

[2] L. Lu, J. D. Joannopoulos, and M. Soljačić, Topological states in photonic systems, Nat. Phys. **12**, 626 (2016).

[3] T. Ozawa, H. M. Price, A. Amo, N. Goldman, M. Hafezi, L. Lu, M. C. Rechtsman, D. Schuster, J. Simon, O. Zilberberg, and I. Carusotto, Topological photonics, Rev. Mod. Phys. **91**, 015006 (2019).

[4] C. W. Hsu, B. Zhen, J. Lee, S.-L. Chua, S. G. Johnson, J. D. Joannopoulos, and M. Soljačić, Observation of trapped light within the radiation continuum, Nature (London) **499**, 188 (2013).

[5] B. Zhen, C. W. Hsu, L. Lu, A. D. Stone, and M. Soljačić, Topological Nature of Optical Bound States in the Continuum, Phys. Rev. Lett. **113**, 257401 (2014).

[6] C. W. Hsu, B. Zhen, A. D. Stone, J. D. Joannopoulos, and M. Soljačić, Bound states in the continuum, Nat. Rev. Mater. **1**, 16048 (2016).

[7] H. M. Doeleman, F. Monticone, W. den Hollander, A. Alù, and A. F. Koenderink, Experimental observation of a polarization vortex at an optical bound state in the continuum, Nat. Photonics **12**, 397 (2018).

[8] Y. Zhang, A. Chen, W. Liu, C. W. Hsu, B. Wang, F. Guan, X. Liu, L. Shi, L. Lu, and J. Zi, Observation of Polarization Vortices in Momentum Space, Phys. Rev. Lett. **120**, 186103 (2018).

[9] W. Chen, Y. Chen, and W. Liu, Singularities and Poincaré Indices of Electromagnetic Multipoles, Phys. Rev. Lett. **122**, 153907 (2019).

[10] J. Jin, X. Yin, L. Ni, M. Soljačić, B. Zhen, and C. Peng, Topologically enabled ultrahigh-Q guided resonances robust to out-of-plane scattering, Nature (London) **574**, 501 (2019).

[11] B. Wang, W. Liu, M. Zhao, J. Wang, Y. Zhang, A. Chen, F. Guan, X. Liu, L. Shi, and J. Zi, Generating optical vortex beams by momentum-space polarization vortices centered at bound states in the continuum, arXiv:1909.12618.

[12] H. Zhou, C. Peng, Y. Yoon, C. W. Hsu, K. A. Nelson, L. Fu, J. D. Joannopoulos, M. Soljačić, and B. Zhen, Observation of bulk Fermi arc and polarization half charge from paired exceptional points, Science **359**, 1009 (2018).

[13] A. Chen, W. Liu, Y. Zhang, B. Wang, X. Liu, L. Shi, L. Lu, and J. Zi, Observing vortex polarization singularities at optical band degeneracies, Phys. Rev. B **99**, 180101(R) (2019).

[14] W. Liu, B. Wang, Y. Zhang, J. Wang, M. Zhao, F. Guan, X. Liu, L. Shi, and J. Zi, Circularly Polarized States Spawning from Bound States in the Continuum, Phys. Rev. Lett. **123**, 116104 (2019).

[15] W. Chen, Y. Chen, and W. Liu, Line singularities and Hopf indices of electromagnetic multipoles, arXiv:1904.09910.

[16] X. Yin, J. Jin, M. Soljačić, C. Peng, and B. Zhen, Observation of topologically enabled unidirectional guided resonances, Nature (London) **580**, 467 (2020).

[17] Y. Kurosaka, S. Iwahashi, Y. Liang, K. Sakai, E. Miyai, W. Kunishi, D. Ohnishi, and S. Noda, On-chip beam-steering photonic-crystal lasers, Nat. Photonics **4**, 447 (2010).

[18] S. T. Ha, Y. H. Fu, N. K. Emani, Z. Pan, R. M. Bakker, R. Paniagua-Domínguez, and A. I. Kuznetsov, Directional lasing in resonant semiconductor nanoantenna arrays, Nat. Nanotechnol. **13**, 1042 (2018).

[19] M. Imada, A. Chutinan, S. Noda, and M. Mochizuki, Multidirectionally distributed feedback photonic crystal lasers, Phys. Rev. B **65**, 195306 (2002).

[20] S. Iwahashi, Y. Kurosaka, K. Sakai, K. Kitamura, N. Takayama, and S. Noda, Higher-order vector beams produced by photonic-crystal lasers, Opt. Exp. **19**, 11963 (2011).

[21] K. Kitamura, K. Sakai, N. Takayama, M. Nishimoto, and S. Noda, Focusing properties of vector vortex beams emitted by photonic-crystal lasers, Opt. Lett. **37**, 2421 (2012).

[22] Z. Hu and Y. Y. Lu, Propagating bound states in the continuum at the surface of a photonic crystal, J. Opt. Soc. Am. B **34**, 1878 (2017).

[23] E. Bulgakov, D. Maksimov, P. Semina, and S. Skorobogatov, Propagating bound states in the continuum in dielectric gratings, J. Opt. Soc. Am. B **35**, 1218 (2018).

[24] X. Gao, B. Zhen, M. Soljačić, H. Chen, and C. W. Hsu, Bound states in the continuum in fiber Bragg gratings, ACS Photonics **6**, 2996 (2019).

[25] J. F. Nye, Lines of circular polarization in electromagnetic wave fields, Proc. R. Soc. A **389**, 279 (1983).

[26] M. Dennis, Polarization singularities in paraxial vector fields: morphology and statistics, Opt. Commun. **213**, 201 (2002).

[27] K. Y. Bliokh, M. A. Alonso, and M. R. Dennis, Geometric phases in 2D and 3D polarized fields: geometrical, dynamical, and topological aspects, arXiv:1903.01304.

[28] J. D. Joannopoulos, S. G. Johnson, J. N. Winn, and R. D. Meade, *Photonic Crystals: Molding the Flow of Light*, 2nd ed. (Princeton University Press, Princeton, NJ, 2008).

[29] See Supplemental Material at http://link.aps.org/supplemental/10.1103/PhysRevLett.125.053902 for (i) the detail of the projected polarization vector, (ii) the analysis with the temporal coupled mode theory, (iii) the analogy between polarization singularities and band degeneracies, (iv) the symmetry consideration of the at-Γ BIC, (v) the mobility of the deterministic off-Γ BIC, and (vi) the comparison with the accidental off-Γ BIC by fine-tuning, which includes Refs. [1,4,5,17,20,25,26,30,31–42].

[30] Y. Guo, M. Xiao, and S. Fan, Topologically Protected Complete Polarization Conversion, Phys. Rev. Lett. **119**, 167401 (2017).

[31] S. G. Tikhodeev, A. L. Yablonskii, E. A. Muljarov, N. A. Gippius, and T. Ishihara, Quasiguided modes and optical properties of photonic crystal slabs, Phys. Rev. B **66**, 045102 (2002).

[32] X. Gao, C. W. Hsu, B. Zhen, X. Lin, J. D. Joannopoulos, M. Soljačić, and H. Chen, Formation mechanism of guided resonances and bound states in the continuum in photonic crystal slabs, Sci. Rep. **6**, 31908 (2016).

[33] S. Fan, W. Suh, and J. D. Joannopoulos, Temporal coupled-mode theory for the Fano resonance in optical resonators, J. Opt. Soc. Am. A **20**, 569 (2003).

[34] H. Zhou, B. Zhen, C. W. Hsu, O. D. Miller, S. G. Johnson, J. D. Joannopoulos, and M. Soljačić, Perfect single-sided radiation and absorption withoutmirrors, Optica **3**, 1079 (2016).

[35] C. W. Hsu, B. Zhen, M. Soljačić, and A. D. Stone, Polarization state of radiation from a photonic crystal slab, arXiv:1708.02197.

[36] S. Fan and J. D. Joannopoulos, Analysis of guided resonances in photonic crystal slabs, Phys. Rev. B **65**, 235112 (2002).

[37] J.-L. Liu, W.-M. Ye, and S. Zhang, Pseudospin-induced chirality with staggered optical graphene, Light Sci. Applications **5**, e16094 (2016).

[38] M. A. Gorlach, X. Ni, D. A. Smirnova, D. Korobkin, D. Zhirihin, A. P. Slobozhanyuk, P. A. Belov, A. Alù, and A. B. Khanikaev, Far-field probing of leaky topological states in all-dielectric metasurfaces, Nat. Commun. **9**, 909 (2018).

[39] N. Parappurath, F. Alpeggiani, L. Kuipers, and E. Verhagen, Direct observation of topological edge states in silicon photonic crystals: Spin, dispersion, and chiral routing, Sci. Adv. **6**, eaaw4137 (2020).

[40] C. Guo, M. Xiao, Y. Guo, L. Yuan, and S. Fan, Meron Spin Textures in Momentum Space, Phys. Rev. Lett. **124**, 106103 (2020).

[41] M. V. Berry, Quantal phase factors accompanying adiabatic changes, Proc. R. Soc. A **392**, 45 (1984).

[42] D. Xiao, M.-C. Chang, and Q. Niu, Berry phase effects on electronic properties, Rev. Mod. Phys. **82**, 1959 (2010).

[43] At-Γ BICs with higher-order charges can be also realized by the accidental merging of several off-Γ BICs {see Figs. 3(c) and 3(d) in Ref. [5]}. Such at-Γ BICs with accidental higher-order charges are not discussed in this Letter.

[44] Y. Cui, J. Zhou, V. A. Tamma, and W. Park, Dynamic tuning and symmetry lowering of Fano resonance in plasmonic nanostructure, ACS Nano **6**, 2385 (2012).

[45] A. C. Overvig, S. C. Malek, M. J. Carter, S. Shrestha, and N. Yu, Selection rules for quasi-bound states in the continuum, arXiv:1903.11125.

[46] S. Iwahashi, K. Sakai, Y. Kurosaka, and S. Noda, Centered-rectangular lattice photonic-crystal surface-emitting lasers, Phys. Rev. B **85**, 035304 (2012).

[47] K. Koshelev, S. Lepeshov, M. Liu, A. Bogdanov, and Y. Kivshar, Asymmetric Metasurfaces with High-Q Resonances Governed by Bound States in the Continuum, Phys. Rev. Lett. **121**, 193903 (2018).

[48] A. S. Kupriianov, Y. Xu, A. Sayanskiy, V. Dmitriev, Y. S. Kivshar, and V. R. Tuz, Metasurface Engineering through Bound States in the Continuum, Phys. Rev. Applied **12**, 014024 (2019).

[49] M. V. Berry, The adiabatic phase and pancharatnam's phase for polarized light, J. Mod. Opt. **34**, 1401 (1987).

[50] K. Konishi, M. Nomura, N. Kumagai, S. Iwamoto, Y. Arakawa, and M. Kuwata-Gonokami, Circularly Polarized Light Emission from Semiconductor Planar Chiral Nanostructures, Phys. Rev. Lett. **106**, 057402 (2011).

[51] A. A. Maksimov, I. I. Tartakovskii, E. V. Filatov, S. V. Lobanov, N. A. Gippius, S. G. Tikhodeev, C. Schneider, M. Kamp, S. Maier, S. Höfling, and V. D. Kulakovskii, Circularly polarized light emission from chiral spatially-structured planar semiconductor microcavities, Phys. Rev. B **89**, 045316 (2014).

[52] S. V. Lobanov, S. G. Tikhodeev, N. A. Gippius, A. A. Maksimov, E. V. Filatov, I. I. Tartakovskii, V. D. Kulakovskii, T. Weiss, C. Schneider, J. Geßler, M. Kamp, and S. Höfling, Controlling circular polarization of light emitted by quantum dots using chiral photonic crystal slabs, Phys. Rev. B **92**, 205309 (2015).

Correction: A byline footnote has been added for the second author.